

## SHAFT VIBRATION OF THE TRUCK

P. Kučera\*, V. Pištěk\*\*

**Abstract:** This article describes analysis of vibrations in a powertrain of a truck with 8 x 8 drive. It may be caused by a deflection of the rotating drive shaft. The aim was to reduce the vibrations, therefore, a transient computational model I for analysis of shaft deflection was created in Matlab software. Analytical and differential equations are used. This model I was compared to the simulation of the transient behaviour of model II with the use of FEM. To verify the computational models, measurements of the shaft deflection and directional vibrations were carried out. The conclusion presents the interpretation of the results of old and new modification of the powertrain and the cause of vibration is also demonstrated.

**Keywords:** Truck, Drive shaft, Vibration, Powertrain, Matlab, Deflection, FEM.

### 1. Introduction

The vibrations affect the drive comfort and may also affect the health of the driver. Therefore, an analysis of the vibrations has become important not only with the passenger cars but also with trucks. The vibrations in trucks may be more intensive and may generate noise. This article deals with the truck vibration. It is a complex dynamic system where the vibrations may occur in any of powertrain parts. These vibrations may be caused by a deflection of the powertrain rotating shaft. The analysed truck showed problems with vibrations and noise after reaching a certain speed. It was documented abroad, where the limits of the European legislations are irrelevant. Therefore, a dependence on the shaft speed and deflection was assumed. To analyse the longest shaft deflection, the transient computational model I was created using analytical and differential equations. Model II uses Finite Element Method (FEM) and this model II works as a check for model I. The validation of the computational models was carried out by several measurements on the truck with 8x8 and 8x4 drive. The directional vibrations and shaft deflection were measured. The conclusion presents results from both the computational models and measured data. This article is based on the literature by Kučera (2015), Waller (1989) and Tůma (2014).

### 2. Computational models

Two computational models of the shaft deflection were prepared. Fig. 1 shows the 3D model of the drive shaft used for the computational model analysis and measuring position.

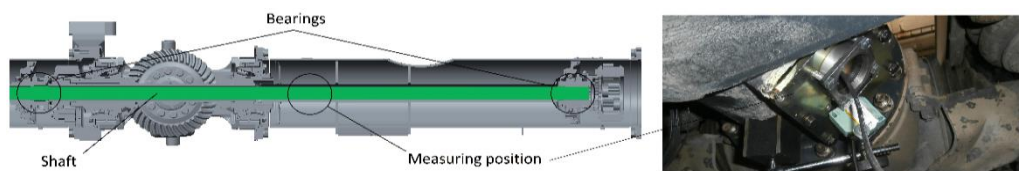


Fig. 1: 3D model of the drive shaft and the measuring position on the right.

First computational model of a rotating shaft with equations based on Budynas (2015) was created. The computational model I of the drive shaft includes the part of the shaft between the two bearings in Fig. 1. This part of the shaft is divided into  $n$  mass points. Number of  $n$  is depended on converge of the task. In this example, there is  $n$  equal to 100. Boundary conditions of the shaft deflection were carried out by the

\* Ing. Pavel Kučera, PhD.: Institute of Automotive Engineering, University of Technology, Technická 2896/2; 616 69, Brno; CZ, kucera@fme.vutbr.cz

\*\* Prof. Ing. Václav Pištěk, DrSc.: Institute of Automotive Engineering, University of Technology, Technická 2896/2; 616 69, Brno; CZ, pistek.v@fme.vutbr.cz

measurement on the truck. This initial deflection was set in the models. The shaft deflection is based on these equations

$$A = A_s / (\sin(L_m \pi / L)), \quad (1)$$

$$r_s = A \sin(x_i \pi / L), \quad (2)$$

where  $A$  is deflection in the middle of the analysed shaft length,  $A_s$  – deflection in the measured position,  $L_m$  – location of measurement,  $L$  – shaft length,  $r_s$  – initial shaft deflection in the individual points dependent on shaft segments and  $x_i$  – coordinates of the shaft section.

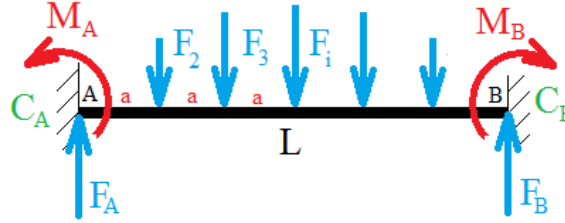


Fig. 2: Forces and torques impacting on the drive shaft model I.

Centrifugal forces act on the individual mass points of the shaft. Their values were determined in each step of the simulation. The following equation was used

$$F_i = m_i r_i \omega_j^2 - F_{i-1}, \quad (3)$$

where  $F_i$  is the centrifugal force in the location of the individual mass points,  $m_i$  – mass of the mass point,  $r_i$  – shaft deflection in the location of the given mass point and  $\omega_j$  – shaft angular speed. It may be assumed that the shaft boundary conditions will be between the hinged and fixed. The most important boundary condition is presented in Fig. 2. It describes the shaft with rotational stiffness in the support.  $M_A$ ,  $M_B$  are the moment reactions and  $F_A$ ,  $F_B$  the force reactions. For the beam with the defined stiffness in the support the force equation, moment equation and two equations (4 – 5) for rotation in points A and B will be used. It is calculated using the Maxwell-Mohr variant of the Castigliano's theorem.

$$\varphi_A = \int_0^L \frac{M_o(x)}{EJ(x)} \frac{\partial M_o(x)}{\partial M_A} dx = -\frac{M_A}{C_A}, \quad (4)$$

$$\varphi_B = \int_0^L \frac{M_o(x)}{EJ(x)} \frac{\partial M_o(x)}{\partial M_B} dx = -\frac{M_B}{C_B}, \quad (5)$$

where  $\varphi_A$ ,  $\varphi_B$  are rotations in points A and B,  $C_A$ ,  $C_B$  – rotational stiffness in the support,  $M_o$  – bending moment,  $E$  – modulus of elasticity, and  $J$  – quadratic moment of the shaft cross-section. To gain values of the deflections in the individual steps, the equation of the deflection line is used. The distance between the mass points is the same as the distance between the forces. The equations of the deflection line are defined as follows

$$EJ\ddot{w} = -F_A x_i + \sum_{i=1}^{n+2} F_i (x_i - (i-1)a), \quad (6)$$

$$EJ\dot{w} = -\frac{F_A x_i^2}{2} + \sum_{i=1}^{n+2} F_i \left( \frac{x_i^2}{2} - (i-1)a x_i \right) + C_q, \quad (7)$$

$$EJw = -\frac{F_A x_i^3}{6} + \sum_{i=1}^{n+2} F_i \left( \frac{x_i^3}{6} - (i-1)a \frac{x_i^2}{2} \right) + C_q x_i + C_{q+1}, \quad (8)$$

where  $i$  is 1, 2, 3,  $n+2$ ,  $q$  is 1, 3, 5,  $n+2$ ,  $w$  is displacement and  $C$  integration constants. These constants have to be determined from the boundary conditions, i.e. the zero displacements in the support. Furthermore, the rotation and deflection values have to be equal between the individual segments. The computational model I is formed in Matlab software. Subsequently, analyses of the 3D parts of the shaft, differential to name but a few were performed using FEM. This computational model II works as a check for model I, therefore, there is no need for detailed description.

### 3. Measurement and evaluation of the directional vibration and computational models

The measurement of the rotating shaft deflections and directional vibrations was carried out with the use of a modular switchboard IMC CRFX 400, card ICPU2-8 and the card CRFX/ISO2-8. Two three-axial

accelerometers, a deflection sensor and a photoelectric reflex switch were used. During the measurement the speed was increased to gain data from the whole span of the truck speed. Subsequently, FFT spectrums, Tuma (2014), of measured vibrations and shaft deflections were interpreted depending on the shaft speed. Scripts to process the data in Matlab software were created. The signal of the shaft rotations is averaged. The measuring position is illustrated in Fig. 1. The speed signal was recorded as a mark per rotation from the photoelectric reflex switch. The measurement of the shaft deflections was carried out by a BAW M30ME-UAC10B-S04G sensor. To measure the drivetrain vibration, two three-axial piezoelectric accelerometers Brüel & Kjær 4524 were used. To interpret the vibration, the FFT analysis from the segment representing the given speed was used. The sample frequency was 20 kHz. From these analyses FFT spectrums were calculated (see in Figs. 3 – 6). The figures show the peak which stands for the 1st shaft speed harmonic order.

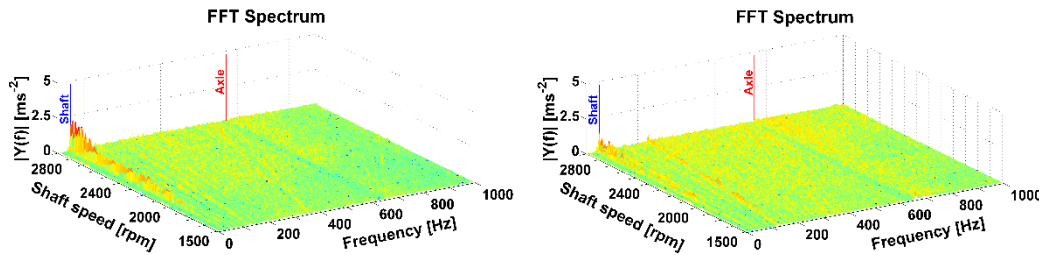


Fig. 3: Analysis of directional vibration – 8 x 4 drive, old and new powertrain (accelerometer 1).

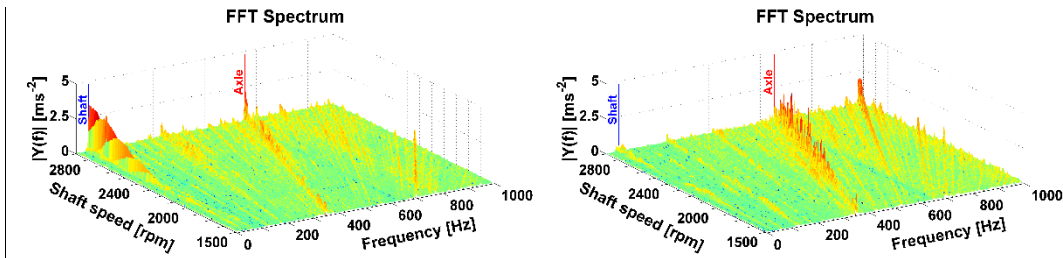


Fig. 4: Analysis of directional vibration – 8 x 8 drive, old and new powertrain (accelerometer 1).

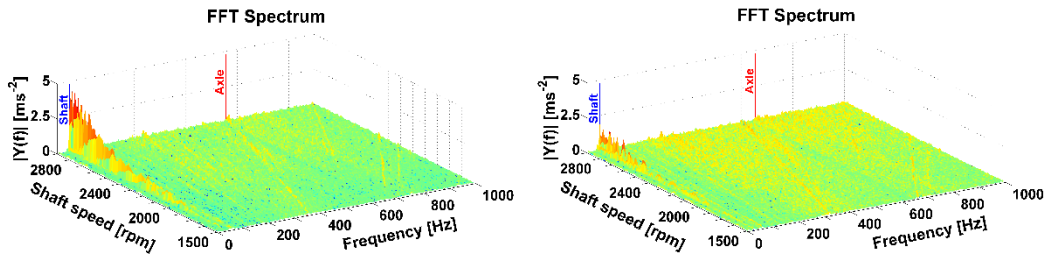


Fig. 5: Analysis of directional vibration – 8 x 4, old and new powertrain (accelerometer 2).

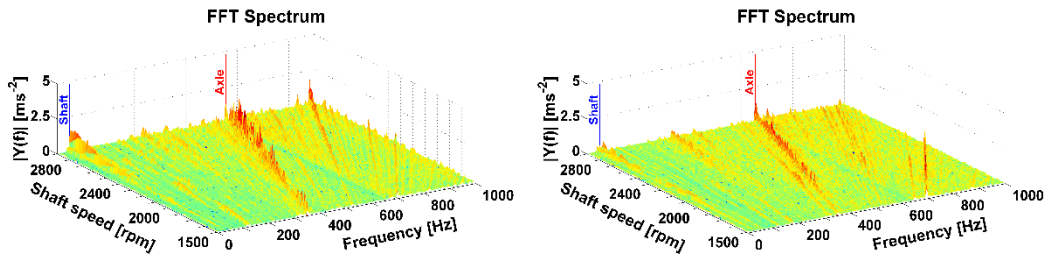


Fig. 6: Analysis of directional vibration – 8 x 8 drive, old and new powertrain (accelerometer 2).

This is the most important factor of the vibration affecting the driver. More peaks occur mainly with the all-wheel drive. But these frequencies are higher than 100 Hz, therefore, it is not important for drive comfort ISO 2631-1 (1997). The comparison of measurements before and after the powertrain modification is also shown. A reduction of vibrations was reached and it is illustrated in Figs. 3 – 6 on the right.

The results of shaft deflection of computational models and measurement are shown in Fig. 7. Other submodels of the model I and II are also compared.

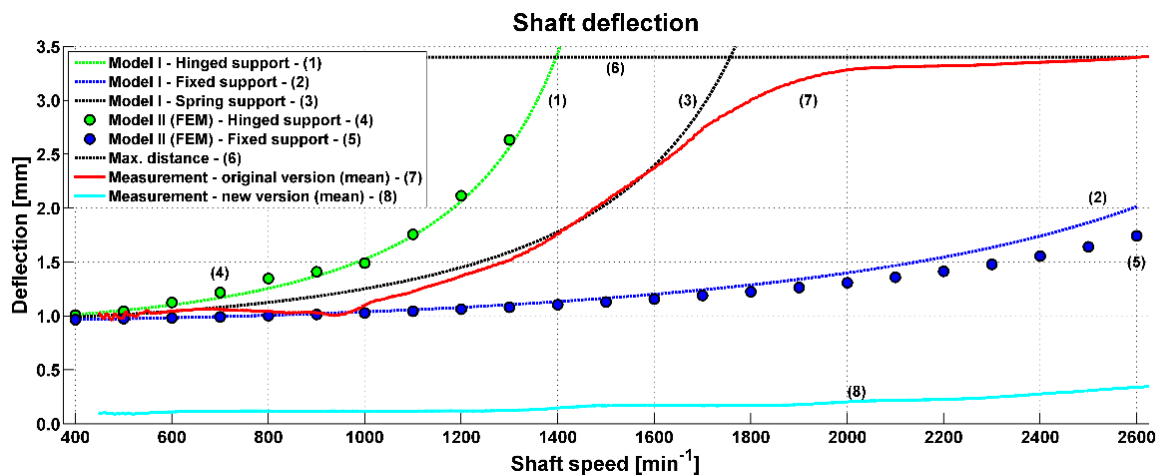


Fig. 7: Comparison of the measured values and computational models.

The measured data were for the span of the shaft rotations in the area of 400 – 2600 min<sup>-1</sup>. These values were averaged and compare with computational models. There is a correspondence of measurement and computational models in the range to 1700 min<sup>-1</sup>. Another section of the graph is different because the deflection is limited in the real shaft (measurement). The shaft deflection limit is 3.4 mm by the dimensions around the shaft. The results of the deflection measurement, vibration analysis and model simulation show that the deflection of this shaft is the main cause of the vibration. To decrease the truck vibration, it was necessary to minimize this shaft deflection. Therefore, a powertrain modification was designed. Two new shafts had been designed and they replaced the original one. These shafts are connected by a special hub with a bearing. The following measurement proved that the shaft deflection was decreased (see curve 8 in Fig. 7 or in Figs. 3 – 6 on the right).

#### 4. Conclusions

There were some problems with vibrations and noise after reaching a certain speed. Therefore, the measurements were carried out. Then their values were compared with the transient computational models and FFT analyses were performed. Based on the results, the computational model I is suitable for another analysis of the shaft deflection. The shaft deflection was reduced by the constructional design. The support of the analysed shaft led to the decrease of vibrations and a near loss of the 1<sup>st</sup> shaft speed harmonic order. This corresponds to the analysis of the directional vibration and 1<sup>st</sup> shaft speed harmonic order is the main cause of the vibrations on the truck. The first computational model may be easily used for the development of the powertrain with long shafts where some deformation or unbalance may occur.

#### Acknowledgement

This work is an output of the internal BUT research project Reg. No. FSI-S-14-2334 and was also supported through NETME CENTRE PLUS (LO1202) by financial means from the Ministry of Education, Youth and Sports under the „National Sustainability Programme I“.

#### References

- Kučera, P. (2015) Mechatronic approach to vehicle dynamics. Doctoral thesis, BUT Brno.
- Budynas, R.G. and Nisbett, J.K. (2015) Shigley's mechanical engineering design. McGraw-Hill Education, New York.
- Waller, H. and Schmidt, R. (1989) Schwingungslehre für Ingenieure: Theorie, Simulation, Anwendungen. BI Wissenschaftsverlag, Zürich.
- Tůma, J. (2014) Vehicle gearbox noise and vibration: measurement, signal analysis, signal processing and noise reduction measures. Wiley, Chichester.
- ISO 2631-1. (1997) Mechanical vibration and shock - Evaluation of human exposure to whole-body vibration - Part 1. Second edition. International Organization for Standardization, Switzerland.